Chapter- 18

Sol-gel Synthesis and Characterization of Lanthanide Modified TiO_2-MCM-41 Mesoporous Materials

K.P. Sreenivasan*, K.R. Anjali, E. Thasneem, P.C. Najeera
Centre for Sustainable Chemical Research, University of Calicut
Approved Research Centre, MES Kalladi College,
Mannarkkad- 678583, Kerala, India
Corresponding author Tel: 9947753498
E-mail address: drsreenivasan@meskc.ac.in

Abstract
In this work lanthanide modified TiO_2-MCM-41 materials have been synthesized by simple sol- gel method. The resultant materials were well characterized by powder X-ray diffraction (XRD), FT-IR spectroscopy, BET analysis, and Transmission Electron Microscopy (TEM). X-ray diffraction analysis indicates that the synthesized materials consist of anatase phase TiO_2. When Ti-MCM-41 was modified by europium, terbium, lanthanum ions there occurs a reduction in crystallinity and crystallite size of anatase TiO_2. The FT-IR spectra TiO_2-MCM-41 showed the presence of Ti-OH, Ti-O-Si and Ti-O bonds. With the addition of lanthanide species several vibrations of TiO_2-MCM-41 have been suppressed. The BET analysis gives information about the surface area and pore size distribution of the materials. The surface area of the TiO_2-MCM-41 has been reduced after incorporation with lanthanide species and is prominent in Tb-TiO_2- MCM-41. The morphology of the materials was clearly investigated using TEM analysis. This study will be helpful for understanding the effect of lanthanide ions on the textural properties of the TiO_2-MCM 41 nanomaterials.

Keywords: Mesoporous materials, Ti- MCM 41, Lanthanide, sol-gel method, textural properties.

ISBN: 9789348505767

1. Introduction

Periodic mesoprous materials are novel materials possess high surface areas, large uniform pore sizes and large pore volumes. These properties make mesoporous materials as attractive candidates for adsorption [1], catalysis [2], drug delivery [3], to fuel cells [4] and sensors [5]. A big advantage of mesoporous materials is that the large mesopores allow for effective transport of reactant and product molecules to and from the active sites, thus modifying diffusion problems that are widely prevalent in microporous materials. Also, the large surface area facilitates the high dispersion of catalytically active sites. In recent years, periodic mesoporous materials have been employed as supports for dispersing photocatalyst materials [6]. These catalysts have been used for photocatalytic degradation of organics, dyes, polluting gases, and splitting of water. Mesoporous materials offer greater flexibility for incorporation of a larger number of photoactive sites. The mesoporous material can be used to limit the size of semiconductors and thus due to quantum confinement effects, the conduction band edge is shifted to more negative values, resulting in a greater thermodynamic potential for the photogenerated electrons for the reduction reaction to produce hydrogen, provide additional pathways for migration of electrons and thus facilitate charge-carrier separation, provide enhanced stability towards photocorrosion. Due to the above mentioned attractive features, mesoporous supports have been employed as catalysts for various applications.

The confinement of TiO_2 crystallites on the silica support promises minimized agglomeration into bulk species and may permit the manipulation of the intrinsic band structure of TiO_2 by shifting the flat band potential in order to achieve greater reduction potentials than bare TiO_2. Lanthanide-containing porous materials have found many applications in various fields. Zhang et al [7] have reported the preparation of lanthanum, gadolinium, and ytterbium doped mesoporous TiO_2 with a series of dopant concentration via sol–gel method without structure-directing agent. Lanthanum-doped mesoporous TiO_2 act as benzene adsorbents [8]. Incorporation of lanthanide ions into a TiO_2 matrix could provide active sites to concentrate an organic pollutant at the semiconductor surface.

ISBN: 9789348505767

Moreover, the incorporation of a doping metal into a mesoporous TiO_2 framework can provide more active sites on the surface of the inside channel, and increase acidity, leading to different physico-chemical properties as well as improved catalytic behavior.

Lanthanide-containing porous materials have found many applications in various fields. Lanthanum-doped mesoporous TiO_2 act as benzene adsorbents and this property depends on two important factors, the doping content and adsorption temperature, on the absorptivity of benzene were investigated [8]. Incorporation of lanthanide ions into a TiO_2 matrix could provide active sites to concentrate an organic pollutant at the semiconductor surface. Moreover, the incorporation of a doping metal into a mesoporous TiO_2 framework can provide more active sites on the surface of the inside channel, and increase acidity, leading to different physico-chemical properties as well as improved catalytic behavior. There are few existing reports, however, focus on surface area effects only, and none to the best of our knowledge have investigated the role of varying lanthanide species on the textural properties of sol –gel derived TiO_2- MCM 41.

Here we report a simple method for the preparation of lanthanide species such as lanthanum, terbium and europium modified TiO_2- MCM 41 material through sol- gel synthesis. The physicochemical properties of the synthesized materials were investigated by powder X-ray diffraction, nitrogen physisorption analysis, transmission electron microscopy, UV-Vis diffuse reflectance spectroscopy, and Fourier transform infrared spectroscopy.

2. Materials methods

2.1 Chemicals

Cetyl trimethyl ammonium bromide (CTAB) (Labochemie), Titanium isopropoxide (Aldrich 98 %), Tetra ethyl ortho silicate (TEOS) (Aldrich), Aqueous ammonia(Nice chemicals),, Isopropyl alcohol, (Nice chemicals), Distilled water.

2.2 Preparation of Ti-MCM 41

0.75 g of CTAB was added to 15 Ml deionised water under vigorous stirring. After CTAB was completely dispersed, 17.5 mL aqueous NH_3 was poured into the clear solution. 22.8 mL of isopropyl

ISBN: 9789348505767

alcohol was added to the surfactant solution under vigorous stirring 30 minutes followed by the addition of 3 mL TEOS and stirring continued for further 10 minutes. The resultant mixture was further treated with 2 ml of titanium isopropoxide and stirred for 24 hours with 300 rpm. The resulting gel was kept for drying at room temperature. Followed by filtration and drying at room temperature calcination was done at 550^0C in a static air environment. The obtained sample was labeled as Ti-MCM41

2.3 Preparation of lanthanide modified Ti-MCM-41

0.75 g of CTAB was added to 15 mL deionized water under vigorous stirring. After CTAB was completely dispersed, 17.5 mL aqueous NH_3 was poured into the clear solution. 22.8 mL of isopropyl alcohol was added to the surfactant solution under vigorous stirring. After stirring for 30 minutes, 3 mLTEOS was added and stirring continued for further 10 minutes and added 2 mL of titanium isopropoxide solution to the resulting mixture. For the preparation of lanthanide modified Ti-MCM-41 o.03 g of Lanthanum (lll) nitrate hexa hydrate, Europium (lll) nitrate pentahydrate and Terbium (lll) nitrate pentahydrate were used as the precursor for lanthanide species. After the addition of lanthanides the stirring was adjusted to 300-600 rpm for for 24 hours. The resulting gel was kept for drying at room temperature. Calcination was done at 550^0C in a static air environment. The obtained samples were labeled as Eu-Ti-MCM-41, Ln-Ti-MCM-41 and Tb-Ti-MCM-41respectively.

2.4 Characterization

The XRD measurements were performed at room temperature using a Rigaku Ultima IV X-ray diffractometer with Cu Kα radiation. The diffractometer was operated at 40 kV, and 44 mA, scanned with a step size of 0.02°, and a count time of 1°/min in the range of 2θ angle 10 to 80. The FT-IR analysis were carried out using a Bruker ALPHA instrument with ATR Pt diamond holder and the spectra were acquired in the range 4000 cm^{-1} to 500 cm^{-1} with a resolution of 4 cm^{-1}.

ISBN: 9789348505767

The TEM images were recorded on a HRTEM Jeol/JEM 2100 instrument operating at 200 kV. Prior to TEM analysis, the sample was dispersed in ethanol and the suspension was sonicated for 1hour. For each material, one drop of suspension was placed on a copper grid coated with carbon film, and allowed to dry overnight. The textural properties, such as surface area and pore size distribution of the materials were analyzed by using N_2 physisorption measurements. After the samples are dried overnight at 70 °C and degas at 200 °C for at least 1 hour, N_2 isotherms are obtained at -196 °C using a BELSORP-max surface area and pore size analyzer. The surface areas of the synthesized materials were calculated by using the Brunauer-Emmett-Teller (BET) equation within a relative pressure range (P/P_0) of 0.05–0.30. The pore volume was determined from the amount of N_2 adsorbed at the highest relative pressure of P/P0 ≈ 0.99. The pore diameter and pore size distribution plots are defined by applying the Barrett-Joyner-Halenda (BJH) model to the desorption isotherm. The UV-Vis diffuse spectra were recorded by a JascoV-550 UV-Visible spectrophotometer with Jasco model ISV 469 reflection accessory

3. Results and discussion

3.1 Powder XRD analysis

The XRD pattern of selected materials Ln-Ti-MCM41, Tb-Ti-MCM41 and Ti-MCM41 are shown in Fig 1. The X-Ray diffraction analysis indicates that the materials exhibit diffraction patterns of amorphous SiO_2 consists of small amount of TiO_2 anatase phase. The peak around 25^o is due to the presence of d_{101} plane of anatase TiO_2 . The intensity of the d_{101} plane was reduced after the modification with lanthanides. This may be due to the lanthanide species blocking the crystal growth of TiO_2 anatase. The peak corresponding to lanthanides are not observed in the XRD pattern, which may be due to the high dispersion of lanthanide ions during sol – gel process.

ISBN: 9789348505767

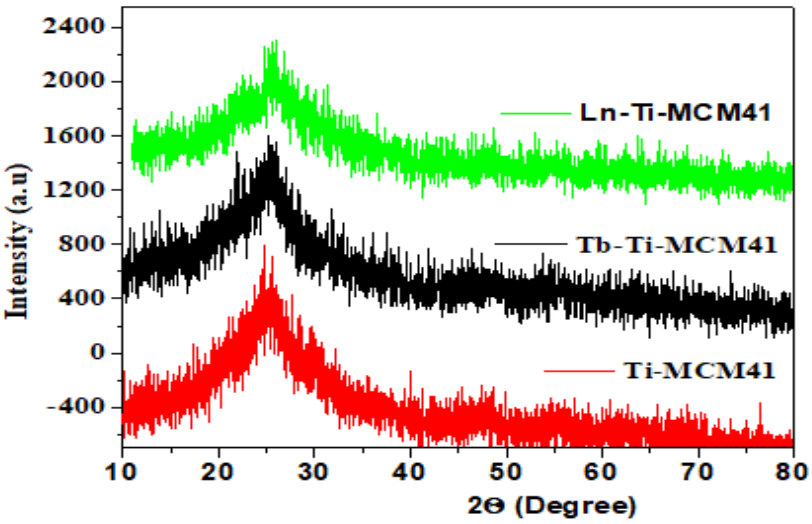

Fig. 1. XRD patterns of Ln-Ti MCM 41, Tb-Ti-MCM 41 and Ti-MCM 41

3.2 FT-IR Analysis

In order to acquire information about the different functional groups, vibrational bands of the materials, we characterized the materials using FT-IR analysis. Fig. 2 showed the FT-IR spectra of Ti-MCM41, Ln-Ti-MCM-41, Eu-Ti-MCM-41and Tb-Ti-MCM41.

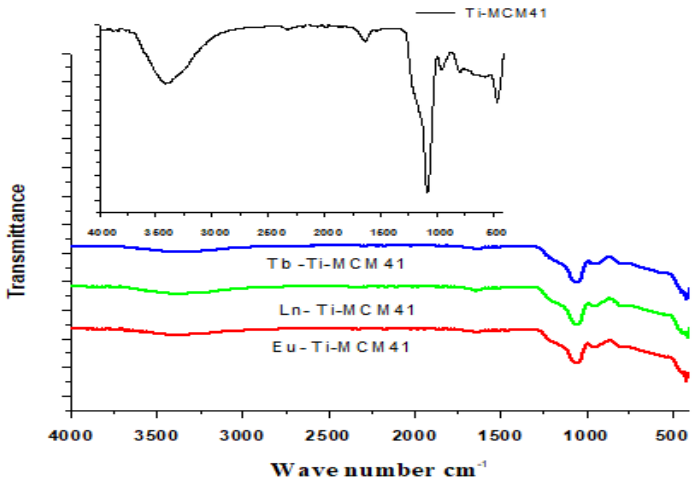

Fig .2 FT-IR spectra of Ti-MCM41, Ln-Ti-MCM-41 , Eu-Ti-MCM-41and Tb-Ti-MCM41

ISBN: 9789348505767

FT-IR spectra of Ti-MCM-41 were shown in the inset of Fig. 2 exhibit a peak at 3450 cm^{-1} corresponding to the presence of -OH group. A small peak at 1623 cm^{-1} shows the presence of Ti-OH bond [9]. Indefinable peaks for Ti-MCM41 within the fingerprint region of the FT-IR spectra there exists a highly intense peak for Ti-MCM41 at 1086 cm^{-1} together with another peak at 483 cm^{-1} which indicates the presence of Ti-O-Si bond [10]. The band covered at the range of 957 to 905 cm^{-1} in the spectrum of Ti-MCM-41 can be ascribed to the stretching vibrations of Ti–O–Si.

Upon modification with lanthanide ions the band at 3450 cm^{-1} broadens. The OH^- ions in the Ti-MCM-41 is partially removed by the lanthanide ions. As the amount of OH^- ions is decreased the intensity of the peak also reduced.

3.3. Nitrogen physisorption studies

Nitrogen physisorption studies were carried out to investigate the surface areas and nature of porosities of the Ti-MCM41 and lanthanide modified Ti-MCM41. The textural properties, including specific surface area, pore volume, and average pore diameter obtained from nitrogen adsorption-desorption analysis, are shown in Table 1.

Table 1: Textural properties of Ti-MCM41, LnTi-MCM-41, TbTi-MCM-41, EuTi-MCM-41

Materials	S_{BET} (m^2g^{-1})	Pore volume (cm^3g^{-1})	Average pore diameter (nm)
Ti-MCM-41	385	0.35	3.65
Ln-Ti-MCM-41	317	0.28	3.54
Eu-Ti-MCM-41	319	0.29	3.61
Tb-Ti-MCM-41	304	0.27	3.62

ISBN: 9789348505767

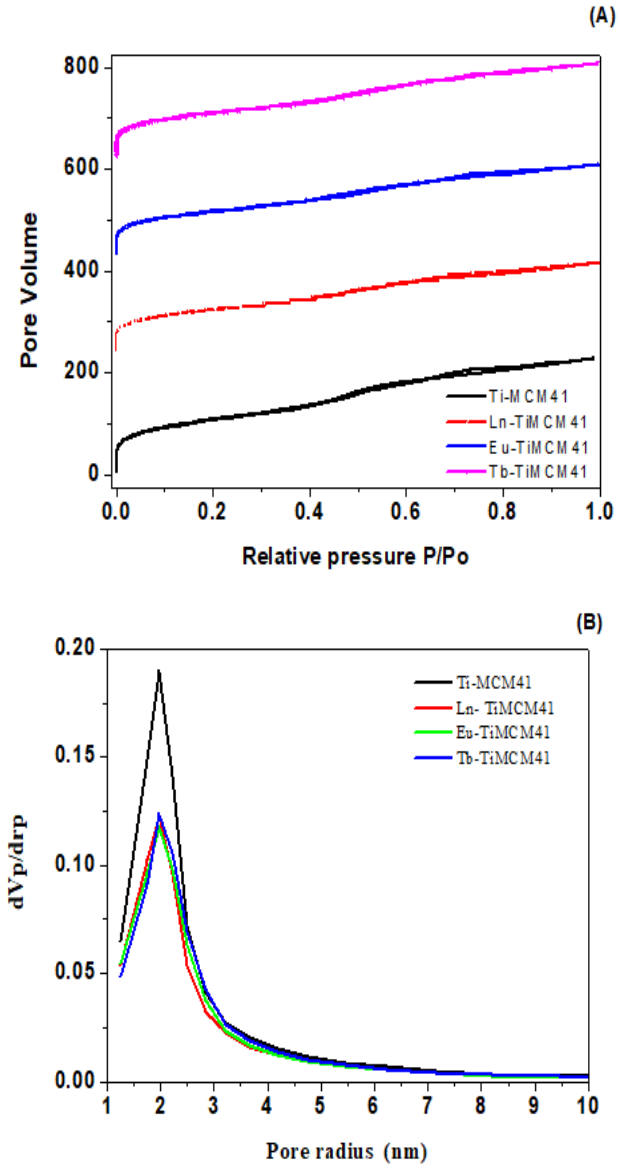

Fig .3 N_2 Adsorption isotherms (A) and Pore size Pore size distribution (B) of Ti-MCM41, Ln-Ti-MCM-41, Eu-Ti-MCM-41, Tb-Ti-MCM-4

The nitrogen adsorption isotherms and the pore size distribution profiles of Ti-MCM41, Ln -Ti-MCM-41, Eu-Ti-MCM-41, Tb-Ti-MCM-41 are shown in Fig.3. The isotherm of Ti-MCM-41 exhibit a typical type IV behaviour with an H4-type hysteresis loop (Fig. 3), which is typical for

ISBN: 9789348505767

mesoporous materials with two-dimensional hexagonal structures [11]. The N_2 uptake at low relative pressure (P/P0< 0.1) for all samples indicates the existence of micropores. The Ti-MCM-41 having the surface area 385 cm^{-1} showing an average pore diameter of 3.65 nm and pore volume 0.35cm^3g^{-1} which is shown in Table 1.

The lanthanide modified materials also exhibit a type IV behavior with an H4 type hysteresis loop. The pore volume and average pore diameter of the species is given in the Table 1. This study indicates that upon modification with the lanthanide ions the surface area of the Ti-MCM-41 has been reduced and is more prominent in Tb-Ti-MCM-41with surface area 304 m^2/g.

3.4 Transmission Electron Microscopic (TEM)

To investigate the internal microscopic structures of the sample, transmission electron microscope analysis were conducted. TEM provides various morphological aspects of mesoporous materials. Fig.4, Fig. 5 and Fig.6 displays various internal structures resulted from parallel and perpendicular penetration of electron beam in the hexagonally arrange channels of mesoporous silicate structures of Ti-MCM-41 , EuTi-MCM41 and LnTi-MCM-41.

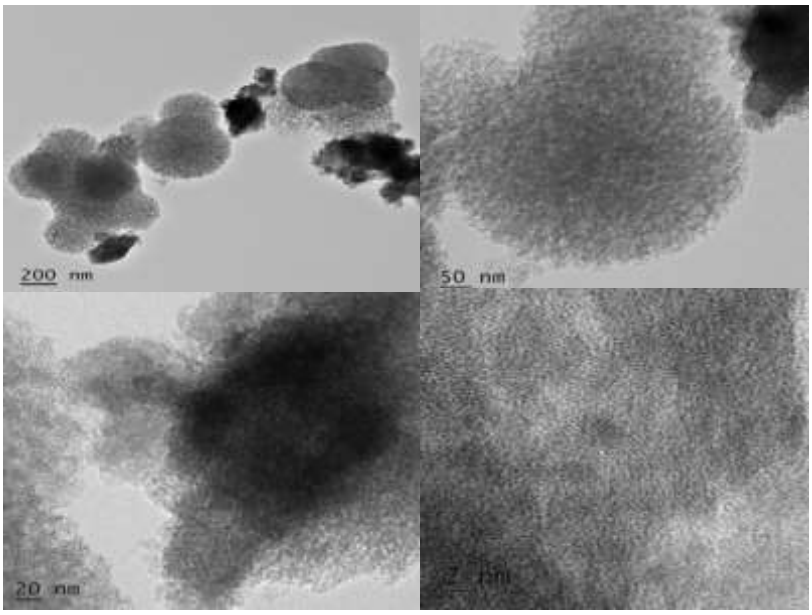

Fig .4. TEM images of Ti-MCM41

ISBN: 9789348505767

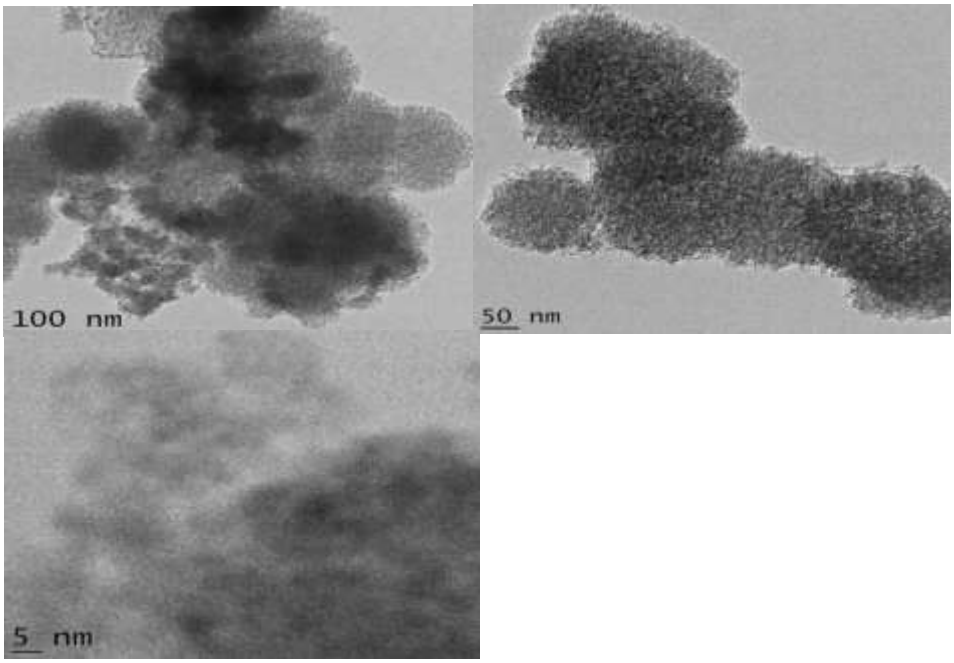

Fig. 5 TEM images of Eu-Ti-MCM41

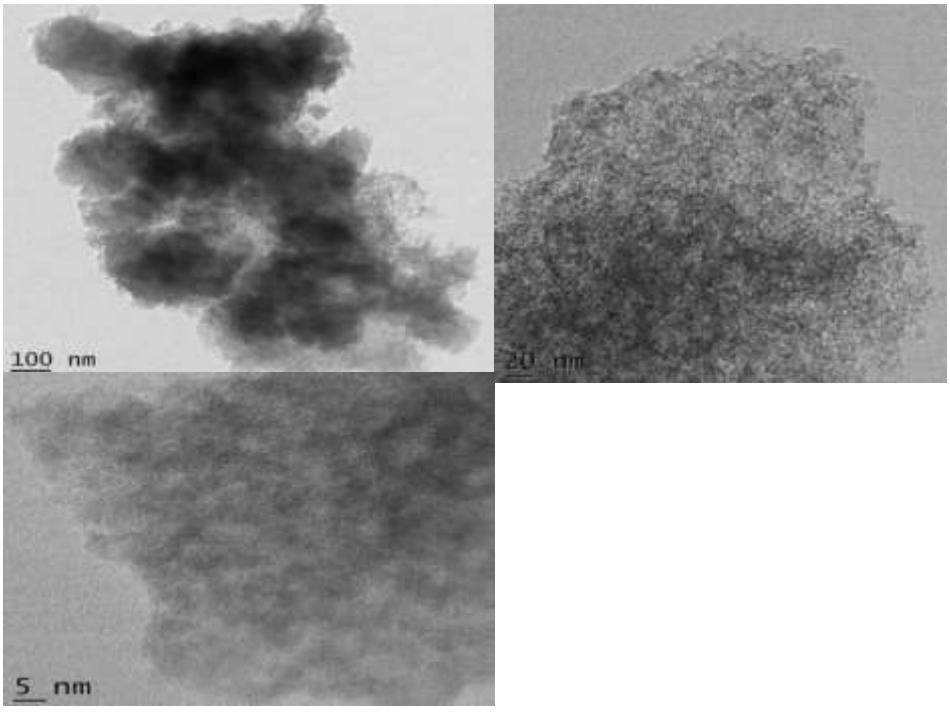

Fig. 6 TEM images of Ln-Ti-MCM41

ISBN: 9789348505767

Conclusion

The Ti-MCM-41 and lanthanide modified Ti-MCM-41 materials were successfully synthesized in by sol-gel method. Different characterization techniques such as XRD, FT-IR, BET, and TEM has been done for each samples and the effect of the lanthanides on Ti-MCM-41 has been studied. X-ray diffraction analysis indicates that the synthesized materials consist of anatase phase TiO_2. When the Ti-MCM-41 was modified by the lanthanide ions like europium, terbium, lanthanum there occurs a reduction in crystallinity and crystallite size of anatase TiO_2. In the FT-IR spectra several characteristic peaks of Ti-MCM-41 can be seen which shows the presence of Ti-OH, Ti-O-Si and Ti-O bonds. With the addition of lanthanides several vibrations of Ti-MCM-41 have been suppressed. The BET analysis gives information about the surface area of the materials. It is clear that the surface area of the Ti-MCM-41 has been reduced with the presence of lanthanides and is prominent in Tb-Ti-MCM-41.The internal structure of the sample is clearly investigated using TEM analysis. The incorporation of lanthanides in Ti-MCM-41 has greatly influenced its characteristics and hence this work provides great opportunity for further research.

Acknowledgement

The authors are thankful to Sophisticated Test and Instrumentation Centre (STIC) for the TEM analysis and Central Sophisticated Instrument Facility (CSIF) for the surface area analysis, and XRD. The authors would also like to acknowledge Miss Sharanya, Research Scholar, MES KVM College, Valanchery for the FT-IR and UV/Visible spectral Analysis.

References

1. P. Zhang, M. He, W.T. Fukuan Li X. Qiu, K. Li , H. Wang, Ordered mesoporous materials for water pollution treatment: Adsorption and catalysis, Green Energy & Environment , 9 (2024) 1239–1256 https://doi.org/10.1016/j.gee.2023.11.001
2. X. Yu, C.T. Williams, Recent advances in the applications of mesoporous silica in heterogeneous catalysis, Catal. Sci. Technol., 12(2022) 5765-5794 https://doi.org/10.1039/D2CY00001F

ISBN: 9789348505767

3. S.Wang, Ordered mesoporous materials for drug delivery, Microporous and Mesoporous Materials, 117 (2009) 1-9 https://doi.org/10.1016/j.micromeso.2008.07.002
4. H. Tang, S. P. Jiang, Self-assembled Pt/mesoporous silica–carbon electrocatalysts for elevated-temperature polymer electrolyte membrane fuel cells, J. Phys. Chem. C, 112 (2008) 19748–19755 https://doi.org/10.1021/jp8066662
5. T. Wagner, S.Haffer, C. Weinberger, D. Klaus ,M. Tiemann , Mesoporous materials as gas sensors,Chem. Soc. Rev., 42(2013) 4036-4053 https://doi.org/10.1039/C2CS35379B
6. R.T. Koodali, D. Zhao, Photocatalytic degradation of aqueous organic pollutants using titania supported periodic mesoporous silica, Energy Environ. Sci., 3 (2010) 608-614 https://doi.org/10.1039/B927247J
7. Y.Zhang, H. Zhang, Y. Xu, Y.Wang , Significant effect of lanthanide doping on the texture and properties of nanocrystalline mesoporous TiO_2, Journal of Solid State Chemistry, 177(2004) 3490-3498 https://doi.org/10.1016/j.jssc.2004.05.026
8. T.D. Nguyen-Phan, M.B Song, E. W. Shin, Removal efficiency of gaseous benzene using lanthanide-doped mesoporous titania, Journal of Hazardous Materials, 167(2009) 75-81 https://doi.org/10.1016/j.jhazmat.2008.12.085
9. C. Ren, W. Qiu, and Y. Chen, Physicochemical properties and photocatalytic activity of the TiO_2/SiO_2 prepared by precipitation method, Sep. Purif. Technol. 107(2013) 264 https://doi.org/10.1016/j.seppur.2013.01.037
10. M. Mokhtarimehr, M. Pakshir, A. Eshaghi, and M. H. Shariat, Super-hydrophilic property of vanadium doped TiO_2–SiO_2 sol–gel derived thin film,Thin Solid Films 532(2013)123 https://doi.org/10.1016/j.tsf.2012.12.104
11. M. Kruk and M. Jaroniec, Gas adsorption characterization of ordered organic–Inorganic nanocomposite materials, Chemistry of Materials, 13 (2001) 3169 – https://doi.org/10.1021/cm0101069

ISBN: 9789348505767